UCRL-9214

UNIVERSITY OF CALIFORNIA

Ernest O. Lawrence Radiation Laboratory

TWO-WEEK LOAN COPY

This is a Library Circulating Copy which may be borrowed for two weeks. For a personal retention copy, call Tech. Info. Division, Ext. 5545

BERKELEY, CALIFORNIA

DISCLAIMER

This document was prepared as an account of work sponsored by the United States Government. While this document is believed to contain correct information, neither the United States Government nor any agency thereof, nor the Regents of the University of California, nor any of their employees, makes any warranty, express or implied, or assumes any legal responsibility for the accuracy, completeness, or usefulness of any information, apparatus, product, or process disclosed, or represents that its use would not infringe privately owned rights. Reference herein to any specific commercial product, process, or service by its trade name, trademark, manufacturer, or otherwise, does not necessarily constitute or imply its endorsement, recommendation, or favoring by the United States Government or any agency thereof, or the Regents of the University of California. The views and opinions of authors expressed herein do not necessarily state or reflect those of the United States Government or any agency thereof or the Regents of the University of California.

UCRL-9214
Limited Distribution

UNIVERSITY OF CALIFORNIA
Lawrence Radiation Laboratory
Berkeley, California

Contract No. W-7405-eng-48

THE DOSIMETRY OF HIGH-ENERGY NEUTRONS PRODUCED BY 6.2-BEV PROTONS ACCELERATED IN THE BEVATRON

Roger Wallace, Burton J. Moyer, H. Wade Patterson,
Alan R. Smith and Lloyd D. Stephens

THE DOSIMETRY OF HIGH ENERGY NEUTRONS PRODUCED BY 6.2 BEV PROTONS ACCELERATED IN THE BEVATRON

Roger Wallace, Burton J. Moyer, H. Wade Patterson
Alan R. Smith, and Lloyd D. Stephens

Lawrence Radiation Laboratory
University of California
Berkeley, California

May 13, 1960

1. Abstract

The high energy neutron flux in the stray radiation field surrounding the Lawrence Radiation Laboratory 6.2 Bev Bevatron is measured by several detector systems of known energy response. The neutron flux as a function of energy is then converted to rad or rem doses by multiplying by the appropriate factors which are a function of energy. Thus the energy response of each detector must be known.

The high energy neutrons in view of their high RBE and low attenuation in the concrete shielding in all locations around the Bevatron consititute the biologically most significant component of the radiation field. Several detector schemes are in use or in a stage of development which are based on the fact that about 6 cm of paraffin surrounding a thermal neutron detector will render its energy insensitive and thus allow a flux determination to be made. For instantaneous flux measurements a BF_3 proportional counter is used inside the paraffin jacket. For integrated fluxes In, Co or Au are used. Threshold detectors of several elements can be used to estimate the neutron spectrum. Polyethylene lined proportional counters whose counting rate is proportional to energy flux are used in conjunction with the energy insensitive detectors to allow the average neutron energy at any detector locations to be calculated. U^{238} and Bi^{209} fission ion chambers of high sensitivity are used to detect the flux of neutrons with energy greater than 1 Mev and 50 Mev respectively. Nuclear track emulsions are used to measure neutron flux and recent developments are directed toward employing them for spectral determinations as well. The synthesis of the data secured from these various detectors into a

(Abstract - cont.)

knowledge of the radiation field intensity and energy distribution in three dimensions as a function of distance from the Bevatron for radiation protection purposes and shielding design will be described.

2. Introduction

The basic methods used in the dosimetry of mixtures of high-energy neutrons and gamma rays at the Lawrence Radiation Laboratory, 6.2 Bev Bevatron in Berkeley, California have been reported at the 1958 Annual International Conference on High-Energy Physics at CERN, Geneva.(1) In this paper several of the ideas presented there will be enlarged upon in the light of recent experience.

3. Basic Method

In evaluating a radiation field consisting of a mixture of neutrons and gamma rays produced by a high-energy accelerator surrounded by concrete shielding, it is important to learn as much as possible about the spectral flux of the neutrons so that the spectrum can be multiplied by the appropriate roentgen biological equivalent (RBE) in order to secure the resulting roentgen-equivalent-man (REM) dose. This operation has been performed in several situations where the spectrum of neutrons was produced by the attenuation of an originally high-energy neutron source.(2) It has been found that although the shapes of the neutron spectra in air and in concrete may be significantly different at energies below 0.10 Mev, this does not strongly affect the neutron dose rate, since by far the largest contribution to the total neutron dose comes from neutrons in the energy interval from 0.10 to 30 Mev. As a result of this fortunate situation, most of our attention is focused on measurements in this latter energy range.

4. Fast Neutron Response of Thermal Neutron Detectors

If a thermal-neutron detector is surrounded by increasing thicknesses of paraffin, its counting rate in a fast-neutron field will increase as paraffin is added, until the paraffin becomes thick enough to absorb the

thermal neutrons more effectively than it produces them from the incident flux of higher energies. After this thickness is exceeded, the counting rate will decrease as more paraffin is added, because of attenuation of the primary neutrons. This build-up and subsequent reduction in counting rate depends on the average energy of the neutrons, as shown in Fig. 1. The energies listed with the five neutron sources were either calculated or measured as indicated. The calculated energies are based on the spectra given by Hess. (3)

It is seen in Fig. 1 that the average energy of an unknown neutron source can be estimated from the shape of its paraffin build-up curve. The error in the counting statistics involved in this set of curves is less than 1%, but an average over a 4π solid angle has been included in the curves, increasing the error to as much as 10%. If these data are converted to counting efficiency as a function of incident neutron energy for various paraffin thicknesses, the curves shown in Fig. 2 are obtained. It is seen that the counting rate of a thermal-neutron detector surrounded by 5 to 7.5 cm of paraffin is independent of the incident-neutron energy within about 30% over the energy range from 20 kev to 14 Mev. The upper curve is for indium foil, while the lower set of curves is for a BF_3 proportional counter. In the case of the BF_3 counter, when 6 cm of paraffin is used inside of a Cd cover, it is seen by interpolation that the counting rate is remarkably constant with neutron energy.

The use of a thermal-neutron detector moderated to constant energy response is not limited to indium and boron. It has been found that cobalt and gold are also quite useful in this technique. The choice of element is based on the time over which it is desired to integrate the dose. This type of detector has the advantage of inexpensive duplication, simultaneity of measurement, and no pile-up problem when used to measure a pulsed source. The foil of the thermal-neutron-capturing element is imbedded in a paraffin sphere 15 cm in diameter, made of two hemispheres. The paraffin sphere has a cavity at its center measuring 3.0 cm in diameter and 0.3 cm deep in which foil can be placed. This assembly is contained in a cubical box 15 cm on a side made of 0.051-cm-thick cadmium. In

the case of indium, the foils are 0.125 mm thick and weigh about 500 mg each.

The indium foils are counted in a methane-flow proportional counter. When activated to saturation in the assembly described above, a foil gives about 4 counts per minute (c/m) for a fast neutron flux of 1 neutron per square centimeter per second (n/cm^2 sec). The counter used at this laboratory has a background counting rate of 10 c/m. A flux as small as 3 n/cm^2sec has been successfully measured with this detector.

Recently cobalt has been used very successfully for long-time surveillance of neutron doses, due to the long half life of Co^{60}.(4) The Co^{60}, produced by thermal neutrons resulting from the moderation of fast neutrons in the paraffin sphere, are counted by a NaI(Tl) gamma-ray spectrometer. Our system is capable of measuring integrated exposures of 10^7 n/cm^2 or more. The lower limit of detectable flux integral is a function of the background counting rate. In the case of each of these detectors, the sensitivity could be increased if a lower-level counting area were available.

5. Energy Flux Density Detector

Another detector that has proved to be very useful is a proportional counter lined with polyethylene. It can be shown that for neutrons that approach it normal to its axis, such a counter has a counting rate which is proportional to their energy flux and not their numerical flux. (5) This situation becomes apparent when an analysis is made of the number of neutrons that produce recoils at varying depths in the polyethylene and subsequently travel far enough into the counting volume to produce a pulse. The validity of this relation between counting rate and energy flux density is based on two assumptions. First, it is assumed that the range of a proton recoil as a function of energy E in polyethylene can be expressed as $R(E) = R_0(E)^{3/2}$. Second, it is assumed that the proton path length in grams per square centimeter in the counter gas necessary for detection is negligible compared to R(E). Since these two assumptions are both good in the range of neutron energies from 0.1 to 20 Mev, true proportion-

ality exists between the counting rate in such a proportional counter and the number of Mev/cm^2 sec available from neutrons in this energy range.

6. Measurement of Average Neutron Energy

By taking the ratio of the counting rate (corrected to Mev/cm^{2}sec obtained with the polyethylene-lined proportional counter to the counting rate in n/cm^2 sec secured with a Bf_3-filled proportional counter surrounded by about 6 cm of paraffin and enclosed in cadmium, one secures the average energy of the neutrons present in a radiation field. This average energy has been found to be very useful in the evaluation of many radiation protection situations. The average energy measured in this manner has been found to agree quite well with that calculated by Hess (3) and estimated from paraffin build-up curves.

7. Variation of Neutron Field with Distance

Recently a series of experiments have been carried out to investigate the neutron field of the Bevatron at large distances. The average neutron energy has been found to be 100 to several hundred kev close to the machine. This value rises to about 400 kev at a distance of 100 m and to 1.5 to 2.0 Mev at 500 m. These values change considerably with different modes of Bevatron operation and also with the asimuthal angle between the tangent to the proton beam at the target position and the location of the neutron counters. The average energy decreases with larger azimuthal angles. The average energies were determined by the ratio method outlined above.

In addition it has been found that the neutron field drops off in proportion to the inverse-square law to within 1% from 100 m to 500 m. Because of the finite size of the Bevatron, the inverse-square law dependence was notfollowed in to closer distances. The inverse-square behavior is consistent with the concept that the neutron field at any distance is determined by the flux of surviving high-energy neutrons for which the attenuation in air is so low in 500 m that it has a small effect. This accounts for the gradual increase in average neutron energy with radius. It is consistent with the findings in many other experiments (6) which indicate that, once equilibrium has been extablished in a particular

medium, from that point on into the medium the spectrum of neutrons is constant in shape, and the attenuation of the whole spectrum is the same as the attenuation of the highest-energy neutrons from which the spectrum is derived by degradation of energy.

8. Neutron Detectors for Use Above 20 Mev

If it is desired to measure the neutrons present in the Bevatron field at higher energies than outlined above, the C^{12} threshold and bismuth fission detectors are very useful. The C^{12} energy threshold is 20 Mev for detecting the C^{12} (n, 2n) C^{11} reaction. This procedure is described by ROGANOV (7) and McCASLIN (8). The energy response is fairly flat from 50 Mev to more than 400 Mev. A 1700-gm piece of plastic scintillator will give 100 disintegrations per minute from its carbon when the neutron flux over 20 Mev prior to counting has been 1 n/cm^2 sec for a period of about three times the 20.4-min half life of the C^{11} formed. The cosmic-ray and natural background counting rate is about 1000 c/m in such a sample. It is possible to secure greater sensitivity by a proper selection of the minimum and maximum pulse heights that are counted and by using an anticoincidence cover of Geiger counters or scintillation counters over the scintillator to reduce the background counting rate.

Another detector for extremely high-energy neutrons with a gradual threshold beginning at 50 Mev is a bismuth-fission ion chamber. The design and mode of operation of such a chamber is described by Hess, et al., (9) where a method is outlined by which it is possible to reduce the electrical capacitance of such a large ion chamber. The bismuth-fission cross section is fairly constant up to as far as it has been measured. (10, 11) The bismuth-fission chamber is as sensitive to high-energy protons, except for their energy losses in its walls, as it is to high-energy neutrons. Such protons are not likely consituents of the radiation field of a large accelerator. The gamma response of the bismuth-fission chamber has been measured and found to be negligible.

9. Low Energy Ion Chambers

Occasionally low-energy ion chambers employing Th^{232} or U^{235} have been used. The U^{235} ion chamber has been found to be especially

useful as a monitor of over-all Bevatron operation. It is placed at the center of the main magnet ring where it views the entire machine equally. In this position its measurement of the thermal-neutron flux is to some extent independent of the particular targets or beam-spill characteristics being employed at the time. The U^{235}-ion-chamber measurements have proved to be well-correlated with circulating-beam-current measurements.

10. Gamma Rays

The gamma-ray dose rates around the Bevatron are measured by a polyethylene-walled ionization chamber and a Lindeman electrometer. It has been found that such an ion chamber agrees with the readings made with a tissue-equivalent ion chamber within a few percent over a large range of gamma-ray energies.

11. Nuclear Track Emulsions

In addition to the use of the several detectors mentioned, the extremely simple procedure of placing nuclear-track-emulsion film badges at various locations in the radiation field for integrated doses is frequently employed. The number of proton-recoil tracks resulting from the neutrons have been found to be independent of the energy over a range from 0.8 to 10 Mev. The sensitivity of the 25-μ thick nuclear emulsion is six to twelve tracks per 245-μ-diameter field of view per REM. Between 0.8 Mev and thermal energy there is a dip in the sensitivity, but at thermal energies the sensitivity is again substantially the same as it is from 0.8 to 10 Mev.

12. Measured Radiation Fields

Many dose measurements have been made near the Bevatron under various operating conditions. (12, 13) Only a brief outline of the results will be given here. Figure 3 shows a radial traverse made by stringing a series of bare as well cadmium- and paraffin-covered indium foils on a radial wire a few feet above the Bevatron. It is seen that the fast-neutron and thermal-neutron fluxes are higher in the center of the machine than they are immediately above the magnet itself. Figure 4 shows a similar traverse made in a circumferential direction. The large increases in dose near the relatively thin-walled tangent tanks labeled WTT, NTT,

ETT, and STT for west, north, east, and south, respectively, are clearly shown, as are target locations and the beam direction.

Figure 5 shows a vertical traverse made with nucleartrack emulsions, hung at 1.5-m intervals about 6-m outside of the shielding blocks. The results do not show a strong shadow of the shielding, but only a gradual increase in the dose with height.

A plan view of the entrance to the west-tangent-tank platform area is shown in Fig. 6. The diagonal lines are drawn to show that a direct view of the tangent wall is possible from the outer floor, and there is an elevation of the dose rate in this area. The reduced neutron production at 4.8 Bev compared to that at 6.2 Bev is shown in most locations. The shielding blocks in the area are indicated, but actually the wall of blocks extends out of the figure at the top and in the lower right-hand corner rather than stopping as shown.

Figures 7, 8, and 9 are circumferential traverses each at two different heights above the floor. It is seen that the dose is conserably reduced in regions immediately outside the shielding (which is schematically represented in an unwrapped form). The slow-neutron flux was measured by a bare BF_3 counter, the fast-neutron flux by a polyethylene-lined proportional counter, and the ionizing radiation by a plastic ion chamber and a Lindeman electrometer.

13. Conclusions

We find that the average neutron energy outside of the shielding is less than 1 Mev and as a result well within the range for which biological data on neutron radiation damage is available. The neutrons are largely produced in evaporation processes and are of low enough energy to be easily eliminated by the first layers of shielding. The few high-energy neutrons produced in stripping, charge-exchange, and knock-on events in the target and walls of the machine are responsible for the main dose outside of the shielding. After these high-energy primaries have entered the shielding, their spectrum is altered, by the addition of low-energy secondaries. At first the secondaries build-up, and then come into equilibrium with the attenuating primaries. The low-energy

secondary neutrons arise from evaporation events in the shielding. After equilibrium is established, i.e. after the peak of the build-up is passed, the neutrons of all energies are attenuated in direct proportion to the attenuation of the primaries, with no further changes in the neutron spectrum. This shift of neutron energy is so effective that the average energy of those neutrons present in biologically significant numbers outside of such a shield is in the neighborhood of 1 Mev.

As a result the most important measurements for biological-dose purposes are made with instruments sensitive in the range of hundreds of kev to a few Mev. Such instruments are easily produced from thermal-neutron-capturing elements contained in a suitable moderator which in turn is surrounded by a thermal-neutron-capturing material. The error in REM dose introduced by ignoring the neutrons above 20 Mev is small.

REFERENCES

1. WALLACE, R., HANDLOSER, J.S., MOYER, B.J., PATTERSON, H.W., PHILLIPS, L., SMITH, A.R., Safety Problems Associated with High-Energy Machines, UCRL-8069, March 1958. Also published in the Proceedings of the Second United Nations International Conference on the Peaceful Uses of Atomic Energy, Geneva, September 1958., Vol. 23, Page 290.
2. PATTERSON, H.W., HESS, W.N., MOYER, B.J., and WALLACE, R., The Flux and Spectrum of Cosmic-Ray-Produced Neutrons as a Function of Altitude, Health Physics 2, 69 (1959).
3. HESS, W.N., Neutrons from (α, n) Sources, Ann. of Phys. 6, No. 2, 115-133 (1959).
4. SMITH, A.R., A Cobalt Neutron Flux Integrator, UCRL-9212.
5. MOYER, B.J., Survey Methods for Fast and High-Energy Neutrons, Nucleonics 10: No. 5, 14 (1952).
6. HESS, W.N., PATTERSON, H.W., WALLACE, R., The Cosmic-Ray Neutron Energy Spectrum, Phys. Rev. 116, 445 (1959).
7. BARANOV, P.S., GOLDANSKII, V.I., and ROGANOV, V.S., Dosimeter for High-Energy Neutrons, Rev. Sci. Instr. 28, 1029 (1957).
8. McCASLIN, J.B., A High-Energy Neutron Dosimeter, Health Physics 2:4.
9. HESS, W.N., PATTERSON, H.W., and WALLACE, R., Delay-Line Chamber has Large Area, Low Capacitance, Nucleonics 15, No. 3, 74-79 (1957).
10. STEINER, H.M. and JUNGERMAN, J.A., Proton-Induced Fission Cross Sections for U^{238}, U^{235}, Th^{232}, Bi^{209}, and Au^{197} at 100 to 340 Mev, Phy. Rev. 101, 807 (1956).
11. SUGARMAN, N., CAMPOS, M. and WIELGOZ, K., Recoil Studies of High-Energy Proton Reactions in Bismuth, Phys. Rev. 101, 388 (1956).
12. SMITH, A.R., The Stray Radiation Field of the Bevatron, UCRL-8377, July 1958.
13. STEPHENS, L.D., and SMITH, A.R., Fast-Neutron Surveys Using Indium-Foil Activation, UCRL-8418, August 1958.

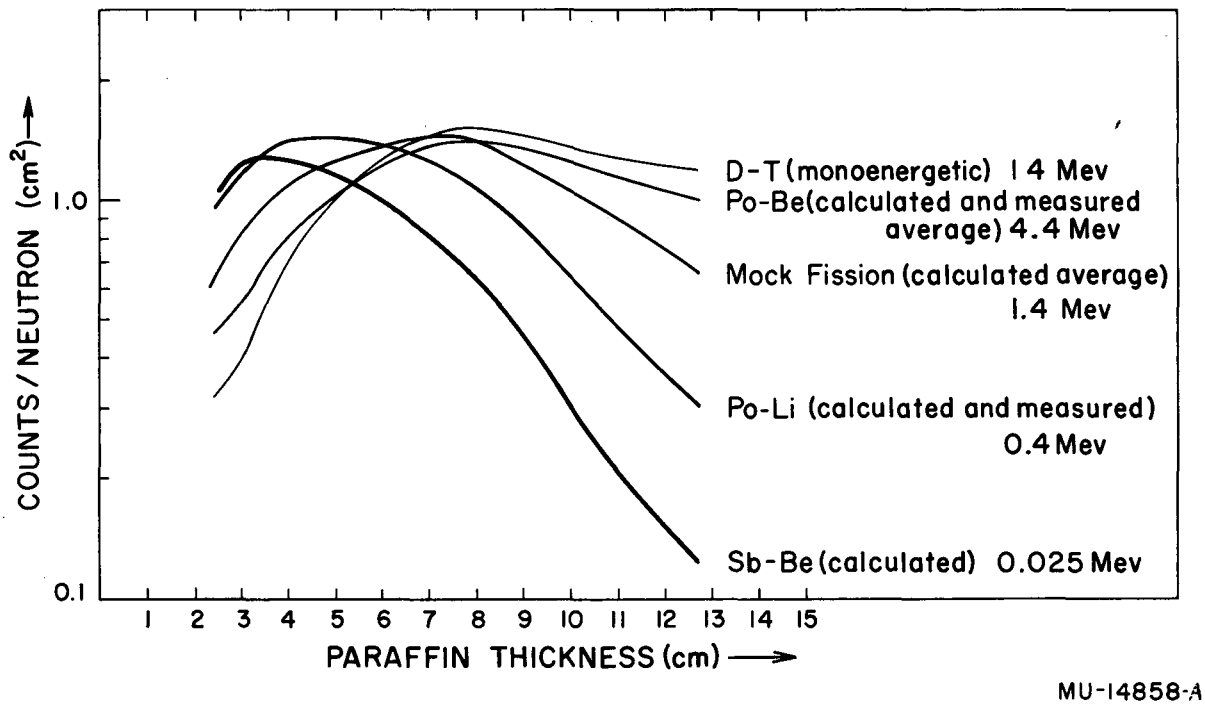

Fig. 1. BF_3 counting rate as a function of paraffin thickness for various neutron sources, corrected to an isotropic flux distribution. The entire assembly was covered by Cd.

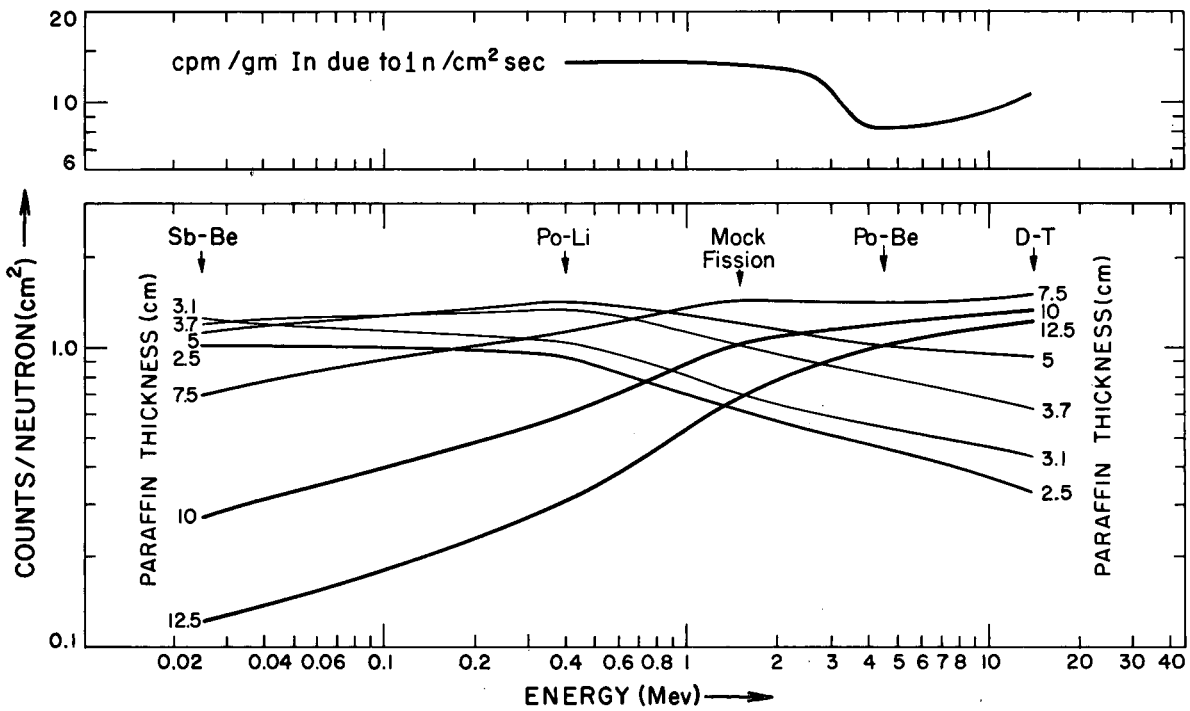

MU-14859-A

Fig. 2. Average efficiency of two thermal neutron detectors as a function of neutron energy for various paraffin thicknesses, corrected to an isotropic flux distribution. The top curve is for In with 7.5 cm of paraffin and the lower curves are for a BF_3 proportional counter. The assemblies were covered by Cd. The averaging over the 4π solid angle has introduced an error of as much as 10 per cent.

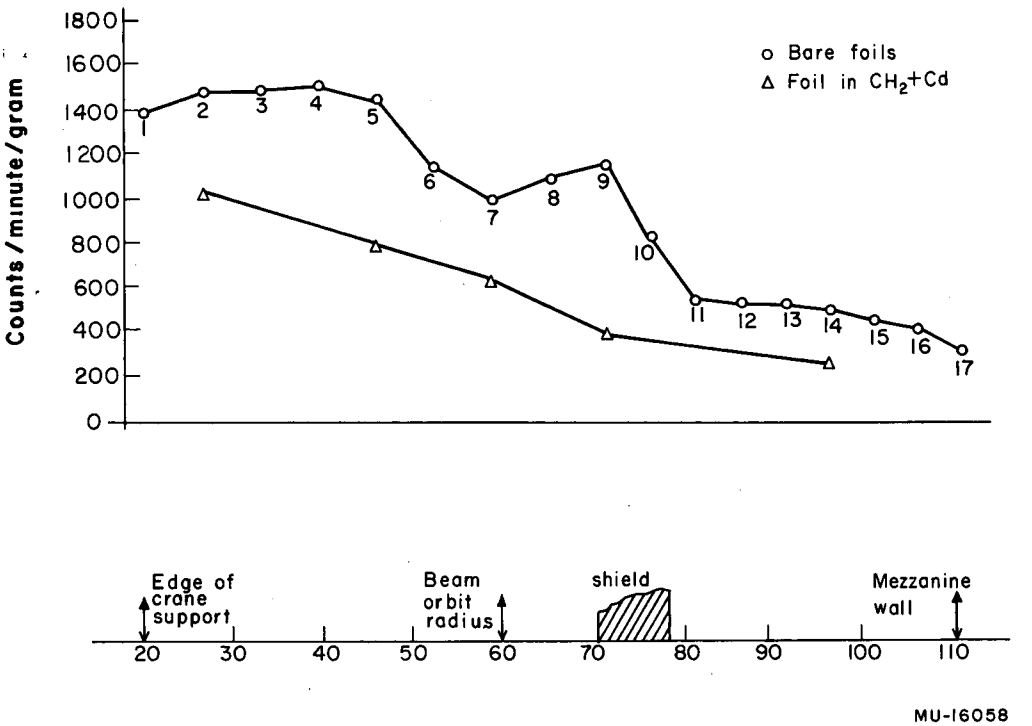

Fig. 3. Indium foil study of neutron flux along a radius at Bay 20. Beam is 2 to 3×10^{10} protons/pulse at 6.2 Bev with 3° carbon target at I_{29}.

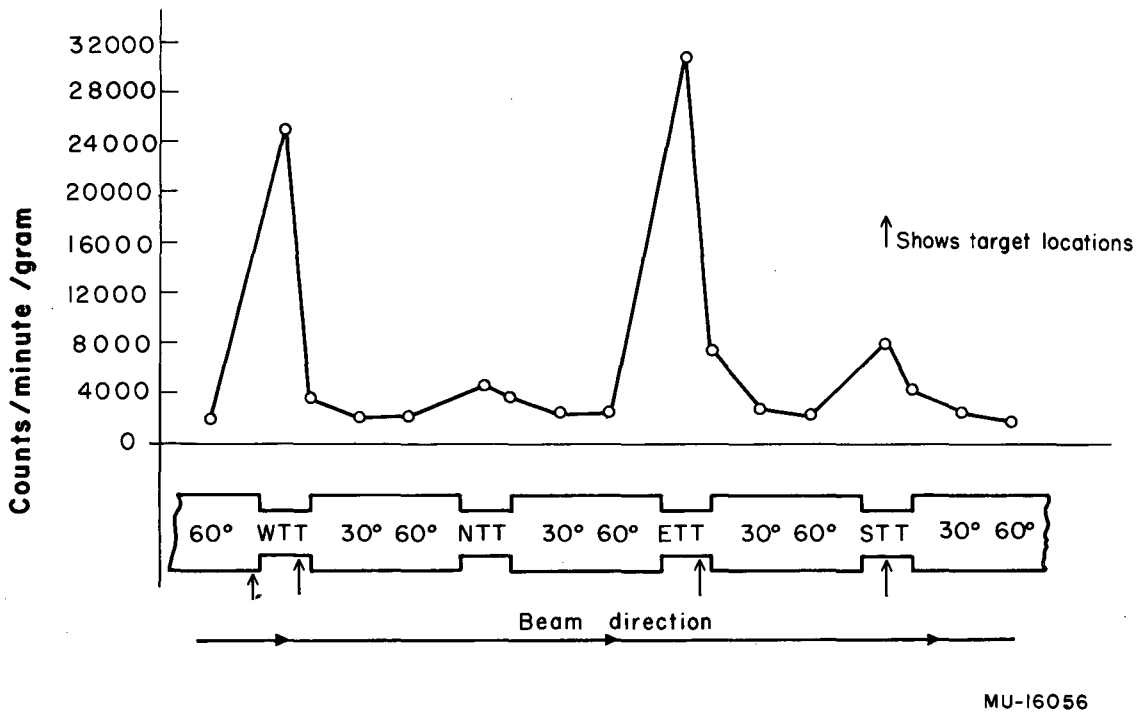

Fig. 4. Indium foil run 3; fast-neutron flux inside the magnet ring. Actual monitor-foil activity: 4480 counts/minute/gram. Beam is $\sim 6 \times 10^{10}$ 6.2-Bev protons/pulse.

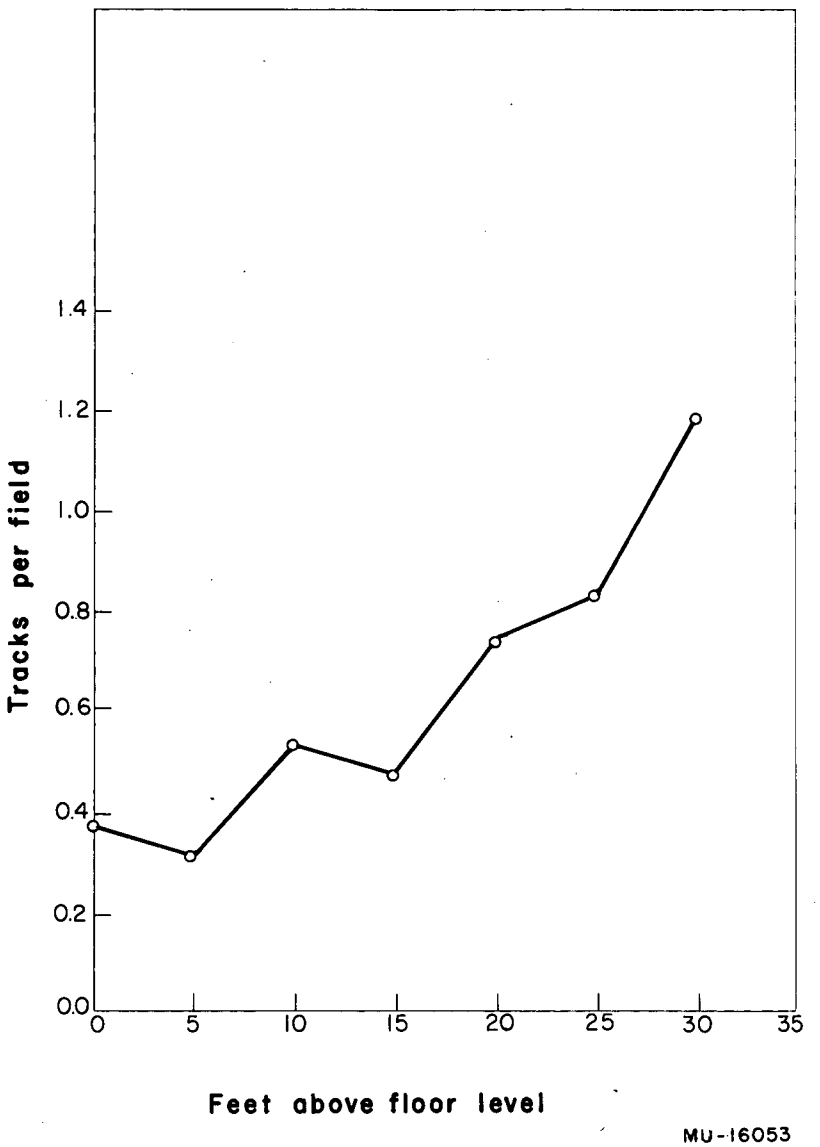

Fig. 5. NTA film study of Bevatron fast-neutron field; elevation survey, Bays 19 and 20.

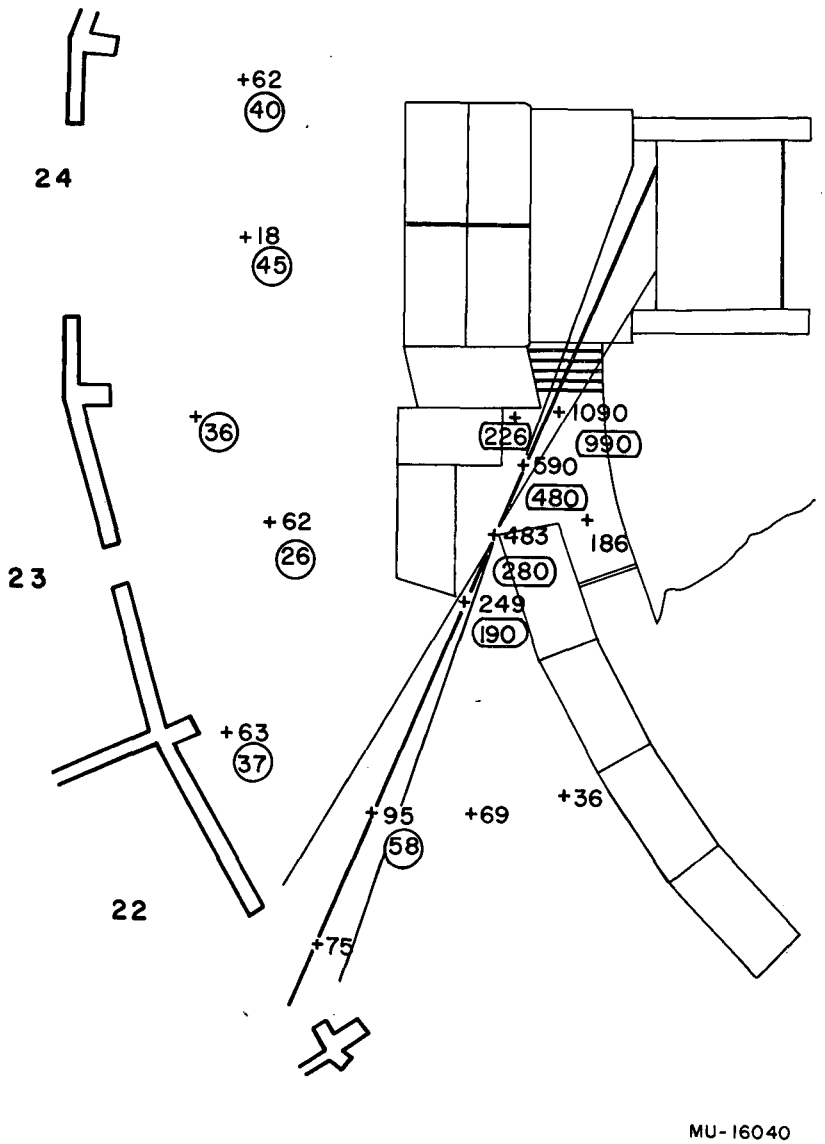

Fig. 6. Fast-neutron energy flux levels for values of E_n between 0.2 and 20 Mev in Mev/cm^2/10^{10} protons for 6.2-Bev protons and 4.8-Bev protons (encircled values) WTT area on Main floor.

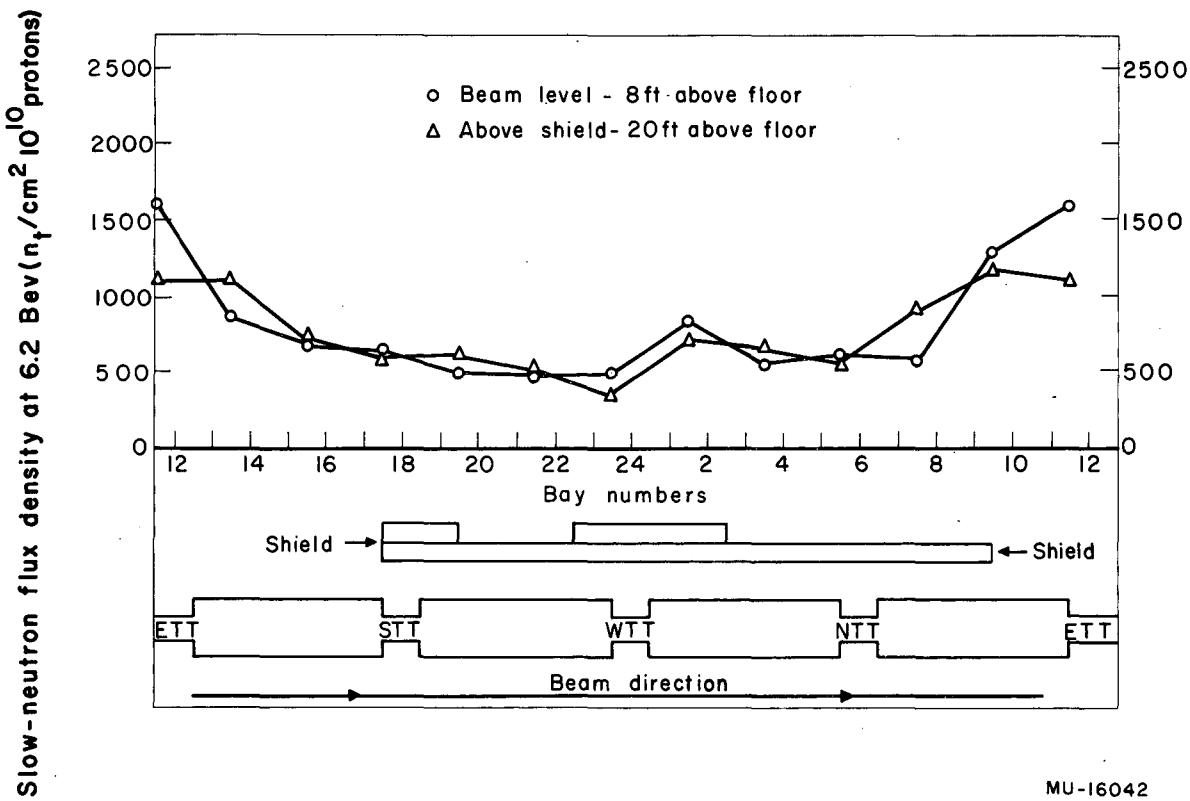

Fig. 7. Three-dimensional survey of slow-neutron flux levels in neutrons/cm^2/10^{10} protons measured at beam level - (8 ft above floor) and 5 ft above shield top. Proton beam energy 5.7 to 6.2 Bev.

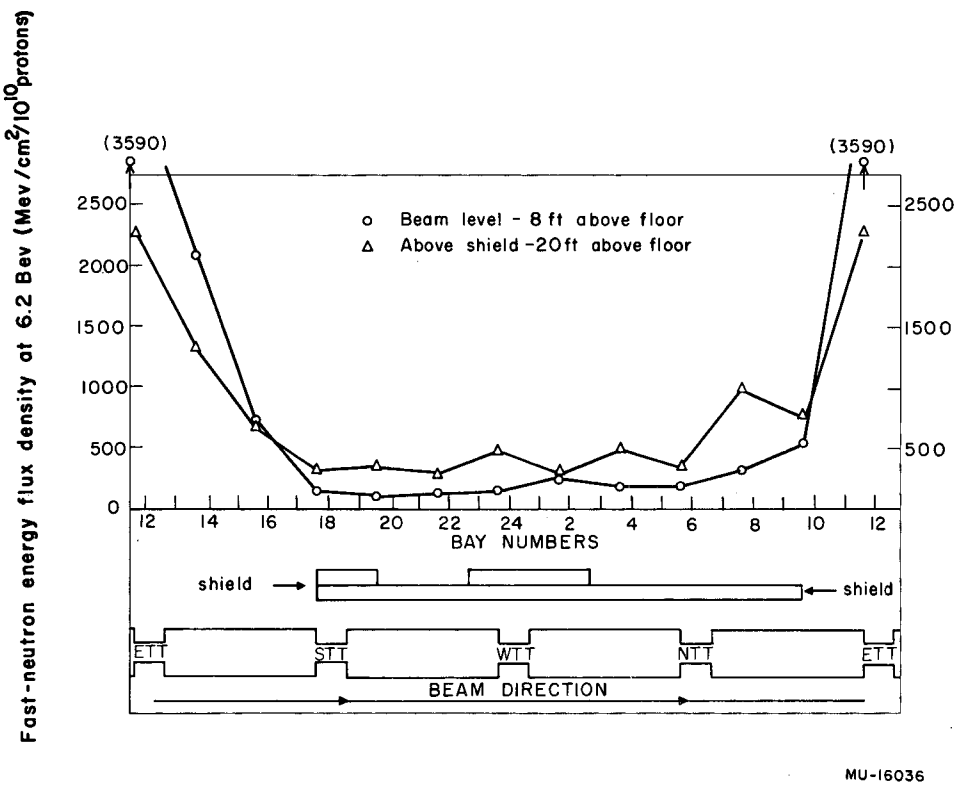

Fig. 8. Three-dimensional survey of fast-neutron energy flux levels for values of E_n between 0.2 and 20 Mev in Mev/cm^2/10^{10} protons measured at beam level (8 ft above floor) and 5 ft above shield top. Proton beam energy 5.7 to 6.2 Bev.

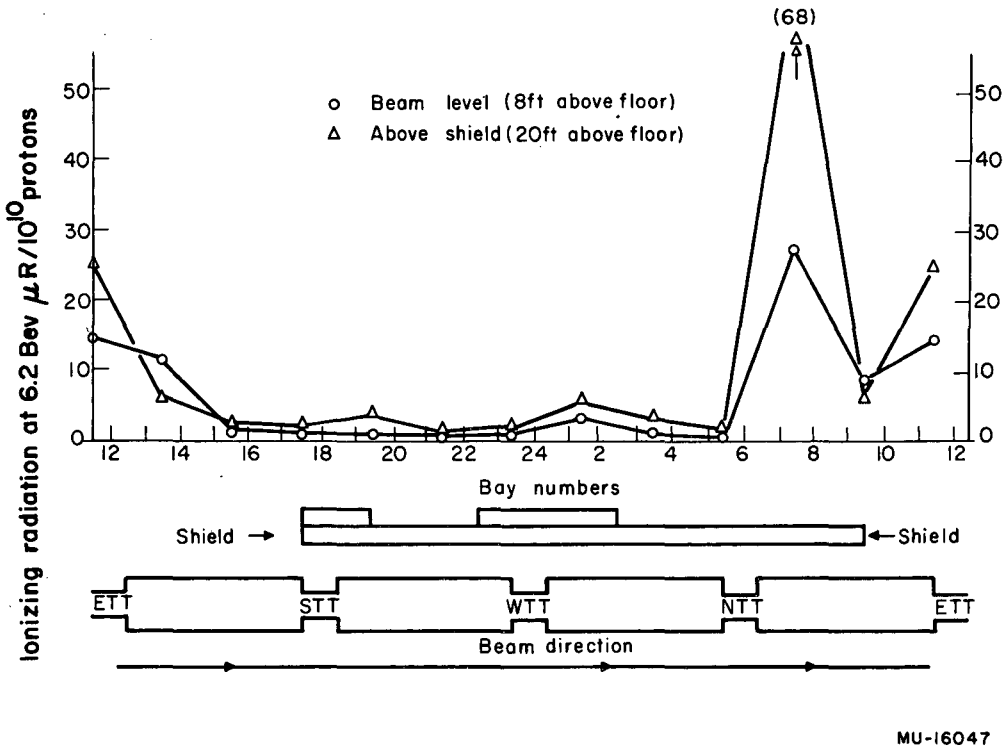

Fig. 9. Ionization-chamber measurements in microroentgens/10^{10} protons at 5.7 to 6.2 Bev. Three-dimensional study at beam level (8 ft level) and 5 ft above shield top.

This report was prepared as an account of Government sponsored work. Neither the United States, nor the Commission, nor any person acting on behalf of the Commission:

A. Makes any warranty or representation, expressed or implied, with respect to the accuracy, completeness, or usefulness of the information contained in this report, or that the use of any information, apparatus, method, or process disclosed in this report may not infringe privately owned rights; or

B. Assumes any liabilities with respect to the use of, or for damages resulting from the use of any information, apparatus, method, or process disclosed in this report.

As used in the above, "person acting on behalf of the Commission" includes any employee or contractor of the Commission, or employee of such contractor, to the extent that such employee or contractor of the Commission, or employee of such contractor prepares, disseminates, or provides access to, any information pursuant to his employment or contract with the Commission, or his employment with such contractor.